The Influence of Inertial Forces on Manual Wheelchair Propulsion

Alberto Amancio Junior[1], **Fabrizio Leonardi**[1], **Agenor de Toledo Fleury**[1,2], **Marko Ackermann**[1]

[1] FEI University, São Bernardo do Campo, Brazil, betoamjr@gmail.com, fabrizio@fei.edu.br, agfleury@fei.edu.br, mackermann@fei.edu.br

[2] Polytechnic School, University of São Paulo, São Paulo, Brazil

Abstract: Both experimental and computational studies have contributed to the understanding of the loads during wheelchair propulsion and the factors leading to the incidence of musculoskeletal disorders. However, few studies have addressed the influence of inertial forces on wheelchair propulsion, which are potentially large as upper limb segments undergo large accelerations along the different phases of the propulsion cycle. This study determines and investigates the influence of inertial forces during manual wheelchair propulsion for a subject at two different locomotion velocities. The isolated influence of inertial as well as gravitational forces is determined using a planar model of the upper extremity and an inverse-dynamics approach. The results show that the inertial forces are preponderant even at the lower speed. These findings evidence that quasi-static models are inappropriate to investigate wheelchair propulsion and show the importance of accurate estimation of anthropometric parameters such as segment masses and moments of inertia, which directly affect inertial force estimations in inverse dynamics-based studies of wheelchair propulsion. The results can also help guide investigations on efficient propulsion techniques, as they show that the radial component of the pushrim forces are, to a large extent, determined by inertial effects rather than by an inefficient propulsion technique .

Keywords: wheelchair propulsion, biomechanics.

INTRODUCTION

According to the World Health Organization (WHO), approximately 1% of the world's population needs wheelchairs. Unfortunately, wheelchair locomotion is an inefficient means of locomotion because of the biomechanics of manual wheelchair propulsion (van der Woude et al., 2001). Furthermore, due to the large and repetitive loads on the upper limbs, the incidence of upper extremity pain and injury in long-term users is high (Veeger et al., 1991). According to Boninger et al. (2002), the most affected area is the shoulder.

Both experimental and computational studies have contributed to the understanding of the loads during propulsion and the factors leading to the incidence of musculoskeletal disorders (Boninger et al. 2002; van der Woude et al., 2001; Veeger et al. 1991; Rankin et al., 2012; Ackermann et al., 2015). Many studies have focused on the reduction of the required demand on the upper limbs for propulsion of the wheelchair by modifying the wheelchair configuration and the propulsion technique (Boninger et al., 2002).

With the increasing accuracy of musculoskeletal models and the growing computational power, computational simulations permit the virtual testing in various scenarios (Rankin et al., 2012 and Ackermann et al., 2015). However, few studies have addressed the influence of inertial forces on wheelchair propulsion, which are potentially large as upper limb segments undergo large accelerations along the different phases of the propulsion cycle (Ackermann et al., 2015).

This study determines and investigates the influence of inertial forces during manual wheelchair propulsion for a subject at two different locomotion velocities (approximately 1.3 m/s and 2.0 m/s). The influence of inertial, gravitational and muscle forces is determined using a planar model of the upper extremity, an inverse-dynamics approach and static optimization. The propulsion patterns are measured in a motion analysis laboratory. The upper limb and wheelchair kinematics are computed from videos acquired by means of a camera and the hand forces by an instrumented pushrim (SmartWheel, www.out-front.com).

METHODS

Mechanical model

We employed a planar multibody model of the upper limb composed of two rigid bodies representing forearm and arm (Fig. 1). The shoulder and the elbow are modeled as ideal hinge joints driven by total active joint moments, τ_s and τ_e, respectively, due to the muscles crossing these articulations. The mass, moment of inertia, center of mass locations and segment lengths are estimated using anthropometric data from a scaled OpenSim model (Holzbaur et al., 2005, Delp et al., 2007) for a 1.69 m, 69.5 kg person, which corresponds to the stature and weight of the subject. The adopted generalized coordinates q are composed by the angle between the upper arm and the vertical, β, the angle between the forearm and the vertical, α, and the horizontal displacement of the wheelchair and shoulder joint, x, as $q = [x\ \beta\ \alpha]^T$. In the propulsion

phase, as in Fig. 1, the hands *P* are in contact with the pushrims and the contact forces F_x and F_y arise, which are measured by the instrumented wheel.

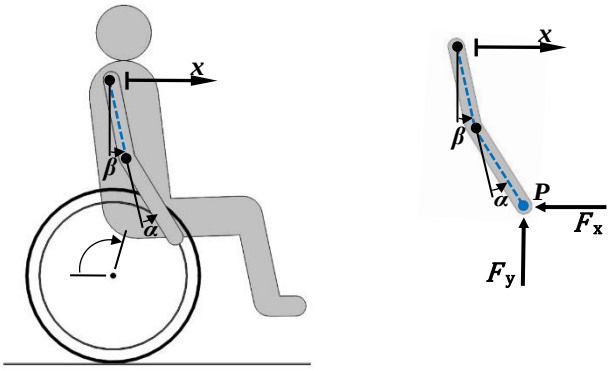

Figure 1 – Upper limb model.

The equations of motion of the wheelchair-user system depicted in Fig. 1 were derived using the Newton-Euler Formalism (Schiehlen, 1997) incorporating the hand-rim contact forces into the equations of motion as

$$M\,\ddot{q} + k(\dot{q}, q) = k_g(q) + G(q)\begin{bmatrix}F_x\\F_y\end{bmatrix} + H(q)\begin{bmatrix}\tau_s\\\tau_e\end{bmatrix}, \quad (1)$$

where *M* is the mass matrix, *k* is the vector of generalized Coriolis and centrifugal forces, k_G is the vector of generalized forces due to gravity, *G* transforms the horizontal F_x and vertical F_y components of the handrim force (Fig.1) in generalized forces and *H* transforms the shoulder moment τ_s and the elbow moment τ_e in generalized forces.

Inverse dynamics

The joint moments, τ_s and τ_e, are computed using inverse dynamics from the measured hand contact forces (F_x and F_y) and upper limb kinematics (q, $\dot{q}$ and $\ddot{q}$) as

$$\begin{bmatrix}\tau_s\\\tau_e\end{bmatrix} = H(q)^{-1}\left(M\,\ddot{q} + k(\dot{q}, q) - k_g(q) - G(q)\begin{bmatrix}F_x\\F_y\end{bmatrix}\right). \quad (2)$$

Musculoskeletal system model

In this study, we used the open biomechanics simulation package OpenSim, which provides a platform for the development and simulation of musculoskeletal models (Delp et al., 2007). We adopted the upper extremity model by Holzbaur et al. (2005). This model has 21 Hill-type muscle models, four of them biarticular, acting across the shoulder and elbow joints. In this analysis, the tendon was considered stiff and the force-length and force-velocity relationships were adopted from Schutte et al. (1993). The muscle force in muscle *i* is

$$Ft_i = a_i\, fl_i\, fv_i \cos(\theta_i)\, Fiso_i = a_i\, k_i\, Fiso_i, \quad (3)$$

where a_i is the muscle activation, fl_i is the force-length relationship, fv_i is the force-velocity relationship, θ_i is the muscle fibers pennation angle, $Fiso_i$ is the maximal isometric force of muscle *i*, and k_i is a modulation factor incorporating the force-length and force-velocity relationships.

Model integration

It was necessary to integrate the OpenSim musculoskeletal model to the mechanical model of the upper extremity implemented in Matlab. Figure 2 shows all the steps necessary to estimate muscle forces along the propulsion cycle using the OpenSim and Matlab models. From the upper limb kinematics data obtained experimentally, the generalized coordinates and their time derivatives ($t, q(\mathrm{t}), \dot{q}(\mathrm{t})\mathrm{e}\ \ddot{q}(\mathrm{t})$) are computed. The joint angles *α(t)* and *β(t)* are used as inputs to the OpenSim program for the computation of the modulation factor of each muscle $k_i(t)$, as well as the muscle moment arm of each muscle with respect to the shoulder $d_{s,i}(t)$ and elbow $d_{e,i}(t)$ along the whole propulsion cycle. OpenSim also provides the maximal isometric muscle force for each muscle $\mathrm{Fiso_i}$. The collected contact forces on the handrim, F_x and F_y, allow for the computation of the joint moments by inverse-dynamics, Eq. (2). Finally, all the information is integrated for the estimation of muscle activations using the static optimization technique (Erdemir et al., 2007).

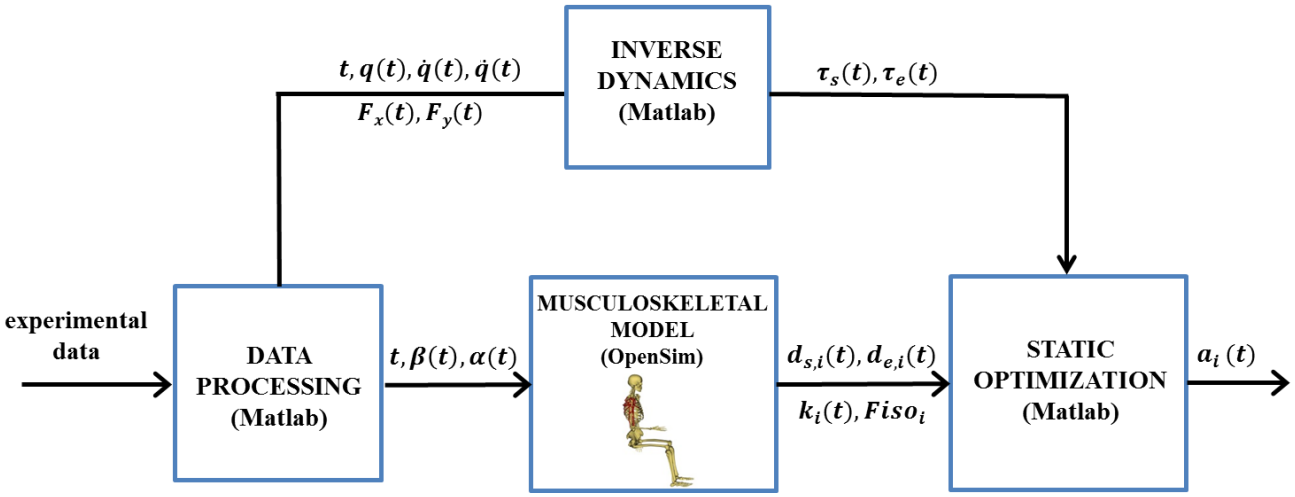

Figure 2 – Block diagram showing steps to estimate muscle forces.

From the moment arms, modulation factors and maximal isometric forces, it is possible to write the shoulder and elbow moments as a function of muscle activations as

$$\begin{bmatrix}\tau_s\\ \tau_e\end{bmatrix} = \begin{bmatrix}d_{O,1}\,k_1\,Fiso_1 & \cdots & d_{O,21}\,k_{21}\,Fiso_{21}\\ d_{C,1}\,k_1\,Fiso_1 & \cdots & d_{C,21}\,k_{21}\,Fiso_{21}\end{bmatrix}\begin{bmatrix}a_1\\ \vdots\\ a_{21}\end{bmatrix} = D\begin{bmatrix}a_1\\ \vdots\\ a_{21}\end{bmatrix}. \quad (4)$$

Estimation of muscle forces

Equation (4) represents a system of 2 equations for 21 unknown muscle activations, which results in the so-called muscle redundancy problem. Assuming the user propels the wheelchair so as to minimize a given performance criterion, the problem of determining the muscle forces or muscle activations can be formulated as an optimization problem, an approach widely used in the literature and named static optimization (Erdemir et al., 2007). According to this approach, the muscle forces/activations are determined by solving the optimization problem in each considered instant of time.

In this study, we adopted the sum of the squared muscle activations as the cost function *J*, which is commonly used in the literature (e.g., van der Helm et al., 1994), as

$$J = \sum_{i=1}^{21} {a_i}^2. \quad (5)$$

The optimization problem is subject to physiological lower and upper constraints on the muscle activations, which ensures muscles are not pushing and do not exceed their maximal force application capacity.

Determining the contributions of inertial, gravitational and muscle forces

In order to estimate the contribution of inertial, gravitational and muscle forces to the handrim forces, we partition the equations of motion, Eq. (1), into three parts (Ackermann et al., 2015) as

$$M\ddot{q} + k(q,\dot{q}) = G(q)\begin{bmatrix}F_{x,i}\\ F_{y,i}\end{bmatrix}, \quad (6)$$

$$0 = k_g(q) + G(q)\begin{bmatrix}F_{x,g}\\ F_{y,g}\end{bmatrix}, \quad (7)$$

$$0 = G(q)\begin{bmatrix}F_{x,a}\\ F_{y,a}\end{bmatrix} + H(q)D\begin{bmatrix}a_1\\ \vdots\\ a_{21}\end{bmatrix}. \quad (8)$$

Note that the sum of these three equations, Eqs. (6-8), results in the equations of motion, Eq. (1), if

$$\begin{bmatrix}F_X\\ F_Y\end{bmatrix} = \begin{bmatrix}F_{x,i}\\ F_{y,i}\end{bmatrix} + \begin{bmatrix}F_{x,g}\\ F_{y,g}\end{bmatrix} + \begin{bmatrix}F_{x,a}\\ F_{y,a}\end{bmatrix}, \quad (9)$$

where $F_{x,i}/F_{y,i}$, $F_{x,g}/F_{y,g}$ and $F_{x,a}/F_{y,a}$ are the handrim forces due to the inertial, gravitational and muscle forces, respectively.

From the perspective of the upper limb joint moments, a similar approach allows for the determination of the individual contributions of the inertial, gravitational and handrim contact forces to the joint moments. Here again the equations of motion

$$\begin{bmatrix}\tau_s \\ \tau_e\end{bmatrix} = H(q)^{-1}\left(M\,\ddot{q} + k(\dot{q},q) - k_g(q) - G(q)\begin{bmatrix}F_x \\ F_y\end{bmatrix}\right) \tag{10}$$

are partitioned into three parts. The contribution of the inertial forces to the shoulder and elbow moments is

$$\begin{bmatrix}\tau_{s_i} \\ \tau_{e_i}\end{bmatrix} = H(q)^{-1}(M\,\ddot{q} + k(\dot{q},q)). \tag{11}$$

The contribution of the gravitational forces to the upper limb joint moments is

$$\begin{bmatrix}\tau_{s_g} \\ \tau_{e_g}\end{bmatrix} = H(q)^{-1}(-k_g(q)). \tag{12}$$

Finally, the contribution of the handrim contact forces to the upper limb joint moments is

$$\begin{bmatrix}\tau_{s_c} \\ \tau_{e_c}\end{bmatrix} = H(q)^{-1}\left(-G(q)\begin{bmatrix}F_x \\ F_y\end{bmatrix}\right). \tag{13}$$

The individual contributions sum up to the total joint moments as

$$\begin{bmatrix}\tau_s \\ \tau_e\end{bmatrix} = \begin{bmatrix}\tau_{s_i} \\ \tau_{e_i}\end{bmatrix} + \begin{bmatrix}\tau_{s_g} \\ \tau_{e_g}\end{bmatrix} + \begin{bmatrix}\tau_{s_c} \\ \tau_{e_c}\end{bmatrix}. \tag{14}$$

Experiments

The experimental protocol was approved by a Brazilian Research Ethics Committee. One 26-year old, male, healthy subject was selected and interviewed about the existence of any previous history of musculoskeletal disorder, injury or pain. In the absence of any of the mentioned conditions and after an explanation of the experimental procedure, the subject gave his informed consent. The subject's weight, stature and other anthropometric measurements were collected. The experiments consisted of two conditions: 1) comfortable, self-selected locomotion velocity on an even surface along a straight distance of about 7.5 m; and 2) fast, self-selected, locomotion on an even surface along a straight distance of approximately 9.5 m. Each test was repeated three times. The subject started from rest and achieved the steady-state condition at about the midpoint of the trajectory. The subject was instructed to keep his trunk motion to a minimum during the trials.

The experiments were performed in the Biomechanics and Motor Control Lab (BMCLab) of the Federal University of ABC, led by Marcos Duarte. The subject propelled a manual wheelchair (Kueschall, Compact 2009 SB 400 mm). The left wheel was replaced by the force measurement system SmartWheel (OUT-FRONT, 2015). The handrim force data was measured at 240 Hz. Reflective, 25 mm markers were placed on anatomic locations (Boninger et al., 1997) and on the wheelchair's wheel (see Fig. 3). Sagittal plane kinematics was collected using a digital camera (BASLER, scA630) at 120 frames per second.

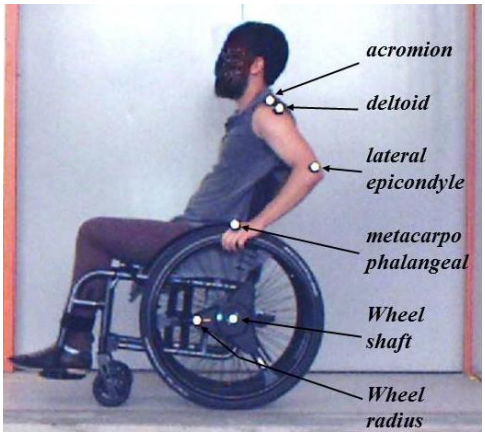

Figure 3 – Reflective markers on the subject and wheelchair.

Data Processing

The recorded videos were processed to obtain the 2D, sagittal plane marker trajectories using the software SkillSpector (video4coach.com/). In order to reduce skin motion artifacts affecting the deltoid marker, the horizontal shoulder joint position x was assumed equal to the horizontal position of the acromion marker. The vertical position of the shoulder joint, in turn, was considered fixed and located 5 cm below the average vertical position of the acromion along the locomotion cycle.

All the date was filtered using a low-pass, fourth-order, zero-lag Butterworth filter with a cut-off frequency of 6 Hz (Boninger et al., 1998, Finley et al., 2004). The sinchronization of the kinematics and handrim force data was performed by comparing the wheel angular position profile provided by the SmartWheel system and the one computed through the wheel markers.

The joint angles β and α (Fig. 1) were computed from the trajectories of the marker positions. The shoulder angle β was obtained from the trajectories of the shoulder joint and the lateral epicondyle marker. The elbow flexion angle α was obtained from the trajectories of the lateral epicondyle and metacarpophalangeal markers. Finally, the first and second time derivatives of the coordinates x, β and α were obtained through finite differences.

RESULTS

Figure 4 shows the upper limb kinematics and the handrim contact force along a complete propulsion cycle in a trial performed at an average speed of 1.3 m/s. The blue and red segments represent the arm and the forearm, respectively. The contact force is represented by the black arrows.

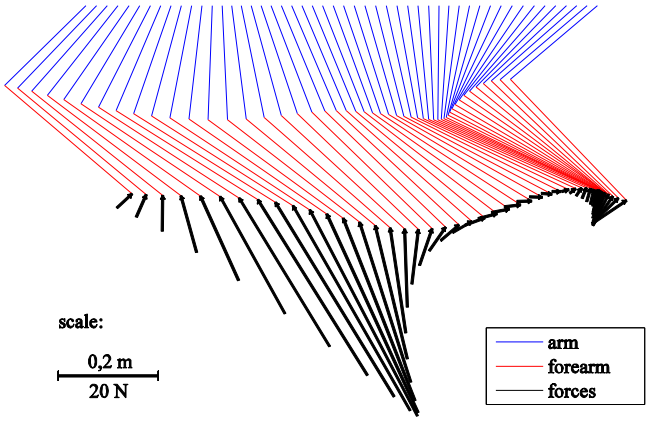

Figure 4 – Graphical representation of upper limb kinematics and handrim contact force along a complete propulsion cycle at an average speed of 1.3 m/s.

Figure 5 shows the individual contribution of the inertial (blue), gravitational (red), contact (green) forces to the total shoulder moment (black) for both locomotion speeds, 1.3 m/s (on the left) and 2.0 m/s (on the right). The reported results represent the average over the three trials for each locomotion speed.

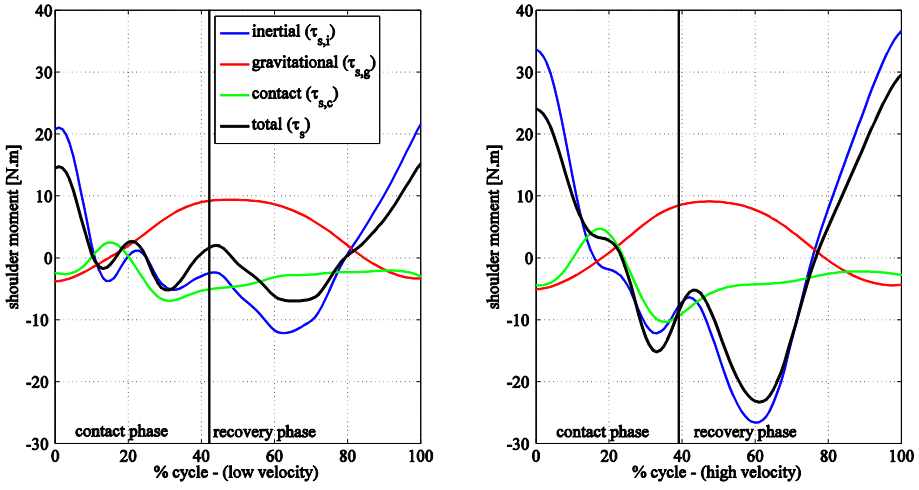

Figure 5 – Individual contributions of the inertial (blue), gravitational (red) and contact (green) forces to the total shoulder moment (black), for the average speeds of 1.3 m/s (left) and 2.0 m/s (right).

Figure 6 shows the individual contribution of the inertial (blue), gravitational (red), contact (green) forces to the total elbow moment (black) for both locomotion speeds, 1.3 m/s (on the left) and 2.0 m/s (on the right). The reported results represent the average over the three trials for each locomotion speed. Note that the contribution of the contact force is not zero in the recovery phase in which the hand is not in contact with the handrim. This occurs because of measuring errors in the SmartWheel system, which provide non-zero contact values at the recovery phase as shown in Fig. 4.

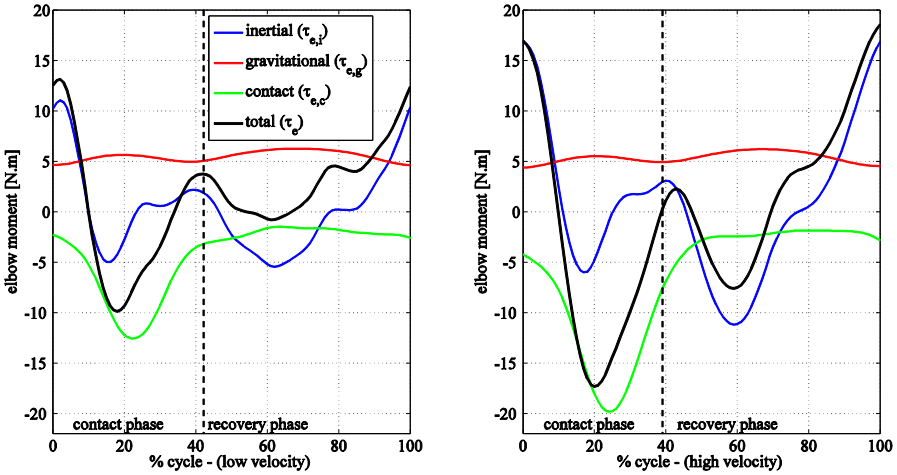

Figure 6 - Individual contributions of the inertial (blue), gravitational (red) and contact (green) forces to the total elbow moment (black), for the average speeds of 1.3 m/s (left) and 2.0 m/s (right).

DISCUSSION AND CONCLUSION

The results show that the inertial forces determine, to a great extent, the profile of the total joint moments, specially of the shoulder, even at the lower locomotion speed. While the gravitational contribution remains almost the same in the two locomotion speeds because it depends exclusively on the upper limb configuration, the inertial forces contribution increases considerably at the larger locomotion speed as accelerations of the upper limb segments increase. It is surprising to observe that the contribution of the handrim contact force to the total shoulder moment is small compared to the contribution of the inertial forces, indicating that a large part of the muscular activity at the shoulder is employed to accelerate the joint segments rather than effectively applying propulsion forces on the handrim.

These findings evidence that quasi-static models (e.g. Leary at al., 2012) are not appropriate to investigate wheelchair propulsion, even at relatively low locomotion speeds. Moreover, these results show the importance of accurate estimation of anthropometric parameters such as segment masses and moments of inertia, as well as measurement of segment accelerations which directly affect inertial force estimations in inverse-dynamics-based studies of wheelchair propulsion.

The results can also help guide investigations on efficient propulsion techniques, as they show that the radial component of the handrim forces, Fig. 4, are, to a great extent, determined by inertial and gravitational effects rather than by an inefficient propulsion technique (Ackermann et al., 2015). This corroborates experimental results by Bregman et al. (2009), according to which instructing wheelchair users to direct propulsion forces tangentially to the handrim led to increased metabolic cost during wheelchair propulsion, i.e. to a less efficient locomotion.

ACKNOWLEDGMENTS

This study was supported by the *National Council for Scientific and Technological Development* – CNPq through the grant MCTI-SECIS/CNPq 458717/2013-4. We would like to thank Marcos Duarte for allowing us to use his lab and acquisition equipment for the collection of the data and Kristy Alejandra Godoy Jaimes for helping with data collection.

REFERENCES

Ackermann, M., Costa, H. R., Leonardi, F. A Modeling Framework to Investigate the Radial Component of the Pushrim Force in Manual Wheelchair Propulsion. In: MATEC Web of Conferences (Vol. 35). EDP Sciences, 2015.

Boninger, M. L., Cooper, R. A., Shimada, S. D., and Rudy, T. E. Shoulder and elbow motion during two speeds of wheelchair propulsion: a description using a local coordinate system. Spinal Cord, v.36, n.6, pp. 418-426, 1998.

Boninger, M. L., Souza, A. L., Cooper, R. A., Fitzgerald, S. G., Koontz, A. M., and Fay, B. T. Propulsion patterns and pushrim biomechanics in manual wheelchair propulsion. Archive Physical and Medical Rehabilitation, v.83, pp.718-723, 2002.

Bregman, D.J.J., van Drongelen, S., Veeger, H.E.J. Is effective force application in handrim wheelchair propulsion also efficient?. Clinical Biomechanics, v. 24, pp.13-19, 2009.

Delp, S. L., Anderson, F. C., Arnold, A. S., Loan, P., Habib, A., John, C. T. and Thelen, D. G. OpenSim: open-source

software to create and analyze dynamic simulations of movement. Biomedical Engineering, IEEE Transactions on, v.54, n.11, pp.1940-1950, 2007.

Erdemir, A., McLean, S., Herzog, W., and van den Bogert, A. J. Model-based estimation of muscle forces exerted during movements. Clinical Biomechanics, v.22, n.2, pp.131-154, 2007.

Finley, M. A., Rasch, E. K., Keyser, R. E. and Rodgers, M. M. The biomechanics of wheelchair propulsion in individuals with and without upper-limb impairment. Journal of Rehabilitation Research and Development, v.41, n.3B, pp. 385-395, 2004.

Holzbaur, K. R., Murray, W. M. and Delp, S. L. A model of the upper extremity for simulating musculoskeletal surgery and analyzing neuromuscular control. Annals of Biomedical Engineering. v.33, n.6, pp. 829-840, 2005.

Leary, M., Gruijters, J., Mazur, M., Subic, A., Burton, M. and Fuss, F. K. A fundamental model of quasi-static wheelchair biomechanics. Medical Engineering & Physics, v. 34, n. 9, pp. 1278-1286, 2012.

Out-Front, 2015. Out-Front: SmartWheel Overview. [Online] Available at: http://www.out-front.com/smartwheel_overview.php [Access on September 22, 2015].

Rankin, J. W., Kwarciak, A. M., Richter, W. M. and Neptune, R. R. The influence of wheelchair propulsion technique on upper extremity muscle demand: a simulation study. Clinical Biomechanics, v. 27, n. 9, pp. 879-886, 2012.

Schutte, L. M., Rodgers, M. M., Zajac, F. E. and Glaser, R. M. Improving the efficacy of electrical stimulation-induced leg cycle ergometry: an analysis based on a dynamic musculoskeletal model. Rehabilitation Engineering, IEEE Transactions on, v.1, n.2, pp.109-125, 1993.

Schiehlen, W., Multibody system dynamics: roots and perspectives. Multibody System Dynamics, v.1, n.2, pp.149-188, 1997.

Van der Helm, F. C. A finite element musculoskeletal model of the shoulder mechanism. Journal of Biomechanics. v.27, pp. 551-569, 1994.

Van der Woude, L. H. V., Veeger, H. E. J., Dallmeijer, A. J., Janssen, T. W. J. and Rozendaal, L. A. Biomechanics and physiology in active manual wheelchair propulsion. Medical Engineering & Physics, v. 23, n. 10, pp. 713-733, 2001.

Veeger, H. E. J., Van Der Woude, L. H. V. and Rozendal, R. H. Load on the upper extremity in manual wheelchair propulsion. Journal of Electromyography and Kinesiology, v. 1, n. 4, pp. 270-280, 1991.

RESPONSIBILITY NOTICE

The authors are the only responsible for the material included in this paper.